Experimental investigation on flame extinction process of non-premixed CH_4/air flames in an air-diluted coflow by CO_2, N_2 or Ar

Jiesheng MIN and Françoise Baillot

Laboratory CORIA – UMR 6614, CNRS-Université et INSA de Rouen, France

1 Introduction

Diluted combustion systems are widely used nowadays, such as: (i) in exhaust gas recirculation combustion systems which are proved to be an effective way to improve combustion efficiency and to reduce pollutant emissions, NO_x; (ii) in fire extinguishment. Phenomena involved in flame stabilization, like liftoff and extinction remain real key points in the control of the diluted combustion. Previous work (Min et al., 2010) highlighted the influence of a diluent addition on flame liftoff phenomena as well as its relative effects between dilution, thermal, and chemistry. This work aims to investigate the influence of different diluents (CO_2, N_2, Ar and CO_2+Ar) on the lifted flame stabilization behavior, as well as the process of flame extinction within a large range of aerodynamic conditions.

2 Experimental Configuration

Experimental set-up is the same as detailed described in (Min et al., 2010). Inside a confined atmospheric vertical square furnace, methane is injected through a round tube with an inner diameter D_i = 6 mm and a burner rim e_l = 2.1 mm. The oxidant, air or air mixed with a diluent inside an upstream blender (CO_2, N_2, Ar or mixture of CO_2+Ar whose heat capacity is the same as that of N_2), enters a stabilization chamber by four inlets. Finally, it flows through the combustion chamber with a 0.25 m side. Quartz windows are installed in two opposite sides of the chamber for visualization needs. Oxidant and methane flow-rate velocities are given in the ranges: $0.1 \leq U_{oxidant} \leq 0.67$ m/s, $1 \leq U_{CH4} \leq 30$ m/s respectively. Gas flows are measured by mass flow meters with an accuracy of 1% full scale. As carefully explained in (Min et al., 2010), it was verified that mechanical impacts due to the way the diluent is added in the air stream do not affect quantities studied here. Flame extinction limits defined hereafter were measured and repeated at least three times. Extinction limit uncertainty varied from 3% to 5% for all diluents. CH* chemiluminescence imaging was used to investigate the flame base in order to quantify how evolves the liftoff height, defined as the standoff distance of the lifted flame above the burner. To do that, direct CH* emission of flame was collected by an Intensified CDD camera (Princeton, 1 fps, 576×384 pixels, 16 bits, exposure time: 250 μs, 0.08 mm/pixel, 50 mm lens) equipped with a band-pass filter, BG-12 which centered at 430 nm with a 50 nm FWHM. As lifted flames present turbulent aspects, no Abel inversion method was applied to instantaneous images. A binarisation process based on the histogram sharp was used to extract the flame foot contour. The

Correspondence to: jiesheng MIN, jiesheng.min@coria.fr

flame base extremity is determined as the first line from the image bottom where the luminous signal is higher than the surrounding noise threshold. The same images were used to calculate the apparent flame radius defined as the distance between the two lateral cuts of the flame base. Results of H_L and R_P are given by the most probable values obtained from 200 images.

3 Flame extinction limit

Flame extinction under no-dilution condition was found impossible under the present operating aerodynamic conditions. In agreement with Muniz and Mungal's extinction diagram (1997), conditions are not strong enough to achieve flame extinction. Therefore, this paper concerns flame extinction obtained only by adding a diluent to the air. On the basis of a previous work concerning flame stability from anchoring to lift-off (Min et al., 2010), extinction experiment campaign has been carried out to complete flame stability charts. Extinction limits have been identified as the ratio $(Q_{diluent}/Q_{air})_{extinction}$ defined by diluent and air flow rates at which flames blow out. First, experiments were carried out for a given diluent to determine how air and methane velocities (U_{air}, U_{CH4}) coupled with dilution to extinguish flames. Results are illustrated with air diluted with CO_2 for U_{air} and U_{CH4} ranging as mentioned above. Diagrams as that one proposed in Fig. 1 show the important role played by the air velocity: extinction limit considerably decreases as U_{air} is increased. Moreover, three types of limits fit data for a given U_{air} : solid lines correspond to the lifting limits, $(Q_{CO2}/Q_{air})_{lifting}$ and dashed ones relate to the extinction limits, $(Q_{CO2}/Q_{air})_{blow\text{-}out}$ by blow-out; dotted lines are the same limits for both lifting and extinction indicating that once flame lifted, no stable lifted flame is available. Thus, dashed lines intersect dotted lines at the methane velocity $U_{CH4,ex}$. It should be noted that curve for U_{air} = 0.1m/s in Fig.1 reports only data for $U_{CH4} \leq$ 15m/s, above which flames tend to approach furnace walls, and it consequently changes operative conditions.

To facilitate the reading, an example obtained at U_{air} = 0.4 m/s is taken as a typical diagram in Fig. 2. It is divided into three regions, each one characterizing a flame state: anchoring at the burner, liftoff, and extinction. When CO_2 is added in the air stream, three scenarios leading to extinction are observed: (i) for $U_{CH4} \leq U_{CH4,ex}$ = 8 m/s, the attached flame lifts off. As no stable lifted flame is available, flame is pushed back continuously and finally extinguishes; (ii) for $U_{CH4,ex} \leq U_{CH4} < U_{CH4,lifting}$ = 14.5 m/s (the value of the lifting point reached in the absence of dilution), the attached flame turns to be a lifted flame before blow-out is achieved; (iii) for $U_{CH4} \geq U_{CH4lifting}$, the flame, initially lifted, blows out by adding a non negligible diluent amount. For $U_{CH4} \geq U_{CH4,ex}$, the unique extinction limit value, $(Q_{CO2}/Q_{air})_{extinction}$ presented in Fig.2 indicates the existence of a characteristic extinction limit for lifted flames under a given U_{air} whatever U_{CH4}. Let us note that lifted flame extinction occurs far away from the burner exit, nearly at the same height about 45 cm for all tested experimental conditions. This height is 2.5 times greater than the one (~ 19 cm) obtained by aerodynamics in a similar non diluted configuration (Muniz and Mungal, 1997). At such a high stabilization position, the mixing flow velocity is greatly reduced because of the large section, and the lifted flame is no longer influenced by the initial methane jet. Thus local flame base curvature radii towards the fresh gases are no longer sharp.

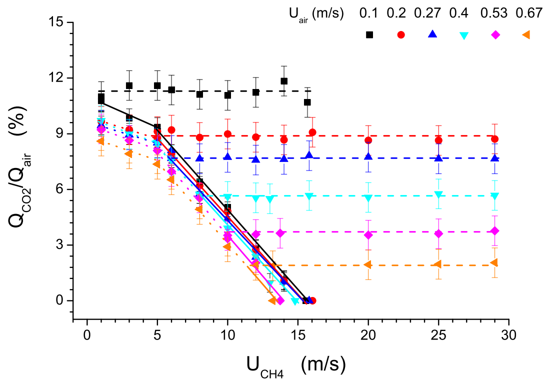

Fig.1 Extinction limits for CO_2 vs. U_{CH4}

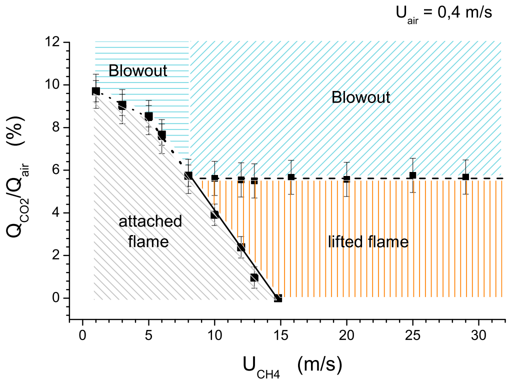

Fig.2 Diagram of extinction limit for CO_2

After gathering all the results, the extinction limit may be presented in the physical space (Q_{CO2}/Q_{air}, U_{CH4}, U_{air}) as a surface, $E_{extinction}$ satisfying $E_{extinction}(Q_{CO2}/Q_{air}, U_{CH4}, U_{air}) = 0$. As seen in Fig. 3, it is composed of a part of the lifting surface $F_{lifting}(Q_{CO2}/Q_{air}, U_{CH4}, U_{air}) = 0$ defined previously by Min et al. (2010) provided that $U_{CH4} \leq U_{CH4,ex}$; for $U_{CH4} \geq U_{CH4,ex}$, $E_{extinction}$ is described by the following equation linearly dependent on U_{air}: $Q_{CO2}/Q_{air} + 0.152\ U_{air} - 0.119 = 0$. $U_{CH4,ex}$ is simply obtained from the phenomenological algebra system: $F_{lifting}\ (Q_{CO2}/Q_{air}, U_{CH4}, U_{air}) = 0$, $Q_{CO2}/Q_{air} + 0.152\ U_{air} - 0.119 = 0$.

The two distinct extinction surfaces highlight the burner rim influence. For flames attached at the burner, the burner rim helps to stabilize their leading edge, described as a propagation kernel by Takahashi and Katta (2000); it prevents the flame from extinction by providing a reduced flow velocity and an inflammable mixture behind the rim by means of a wake structure. This is consistent with the work of Otakeyama et al. (2009) concerning flame stabilization mechanisms. Therefore, for $U_{CH4} \leq U_{CH4,ex}$, flames, still anchored, present a "delay" in extinction compared to flames in the liftoff state. The fact that attached flames extinguish at a higher extinction limit, due to the rim protection, than the aforementioned characteristic extinction limit, induces an immediate flame-extinction just after their liftoff.

The linear dependence of the extinction limit on U_{air}, given by the above parametric equation, can be explained by the stabilization process of a lifted flame inside a coflow jet: lifted flames stabilize inside the mixing region where a suitable flow velocity and an inflammable mixture can be simultaneously found (Cessou et al., 2004). Therefore, increasing U_{air} induces a global augmentation of the flow velocity inside the mixing region. As a result, to maintain flames lifted in the vicinity of an extinguishment limit, the diluent amount has to be decreased to obtain a higher flame burning velocity, S_L characterizing propagating flame edge dynamics. Through this way, the balance between flow velocity and S_L necessary to stabilize flames can be renewed. Meanwhile, as shown by Wyzgolik and Baillot (2007), a small increase of U_{air} greatly influences the jet mixing layer, and in particular its vortical structures in the near field, which plays a crucial role in lifted flame stabilization. Besides, the extinction plateau obtained for $U_{CH4} > U_{CH4,ex}$ indicates that methane velocity has no influence to extinguish flames once lifted, when diluent is added in the air side. Since lifted flame extinction occurs far away from the burner exit, region of complete mixing between methane and air, for a turbulent coflow jet, is achieved at this height. Thus, increasing U_{CH4} leads to a negligible local flow velocity modification because of the large furnace section and of the substantial air flow rate. Finally, mixing between air and the augmented methane flow, results a slight change in the spatial concentration field. By adjusting their liftoff height and radius, flames stabilized inside this complete mixing region can find a location where suitable local flow velocity and mixture conditions are simultaneously ensured. Therefore, the methane velocity increase, leading to a minor effect inside the complete mixing region developing far away from the burner exit, does not influence the extinction limit.

Influence of the nature of a diluent has also been studied by using three other diluents: N_2, Ar, and the CO_2+Ar mixture whose molar heat capacity equals that of N_2. Results are illustrated for the case U_{air} = 0.1 m/s in Fig. 4. The relative order between extinction limits measured with the different diluents is the same as that ordering liftoff limits (Min et al., 2010). This means diluents modify flame extinction

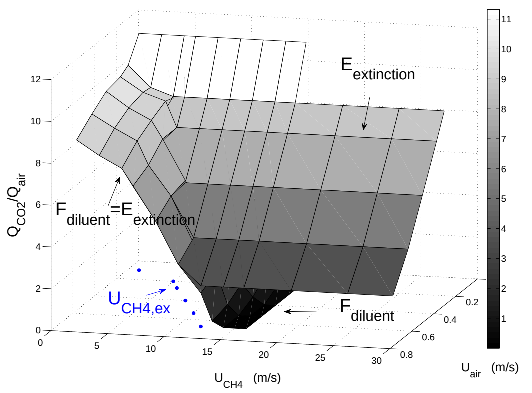

Fig. 3 Surfaces $\mathcal{F}_{diluent}$ and $\mathcal{E}_{extinction}$

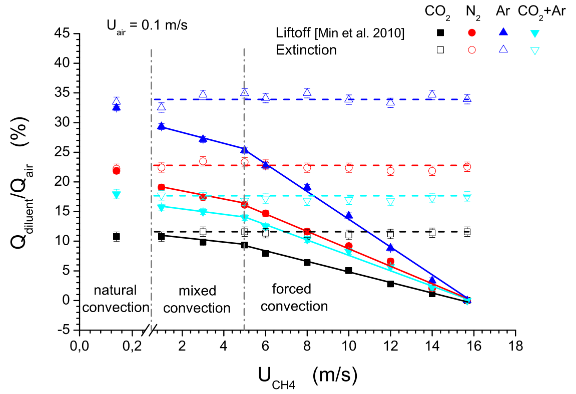

Fig. 4 Extinction limits vs. U_{CH4} for 4 diluents

processes similarly to flame lifting processes which were shown to be influenced through three main effects (dilution, thermal and chemistry) by Guo et al. (2010). Thus, a new parameter, $K_{diluent}$ which characterizes the capability of a diluent to break flame stability relative to that of CO_2, is jointly defined for the two processes as follows: $K_{diluent} = (Q_{diluent}/Q_{air})_{extinction}/(Q_{CO2}/Q_{air})_{extinction} = (Q_{diluent}/Q_{air})_{lifting}/(Q_{CO2}/Q_{air})_{lifting}$. Values of $K_{diluent}$ for diluents studied in this work are found to be equal to $K_{CO2} = 1$, $K_{N2} = 1.9$, $K_{Ar} = 2.9$ and $K_{CO2+Ar} = 1.6$. As found in $F_{lifting}$ surface (Min et al., 2010) for $U_{CH4} \leq U_{CH4,ex}$, a unique extinction parametric equation written with $K_{diluent}$ is established for describing $E_{extinction}$ surface: $(Q_{diluent}/Q_{air})/K_{diluent} + 0.152\ U_{air} - 0.119 = 0$, for $U_{CH4} > U_{CH4,ex}$. Therefore, flame extinction limits for other diluents can be deduced from those of CO_2, once $K_{diluent}$ is known.

4 Flame liftoff height and radius

The liftoff height, H_L (H_L^o with no dilution) is used to characterize lifted flame stability. In the no-dilution case (see figure 5), liftoff height increases with U_{CH4} increase. The influence of U_{air} is quite limited in the range $0.1 \leq U_{air} \leq 0.27$ m/s whereas an offset in the H_L curve is found at $U_{air} = 0.4$ m/s. This is similar to what was observed by Wyzgolik and Baillot (2007). This abrupt increase is piloted by the edge flame dynamics and its burning velocity. Indeed, as mentioned above, lifted flames stabilize in the mixing region where a suitable flow velocity can be found to balance its propagation speed, close to 0.4 m/s here. Once U_{air} is greater than this value, lifted flames are not able to find a position in the near field where flow velocities are comparable to the flame propagation speed. Thus lifted flames move farther downstream where the methane-oxidant mixing velocity is locally reduced. This heuristic explanation was already confirmed by Wyzgolik and Baillot (2009) through a N_2-diluted air for which an abrupt increase of the lifted flame started at $U_{air} = 0.2$ m/s, a value equal to the flame burning speed of the associate stoichiometric mixing.

Adding a diluent decreases the reaction rate through three ways (pure dilution, thermal and chemical effects), which induces a reduction of S_L (Qiao et al., 2010). Thus lifted flames being pushed backwards, H_L is increased. Here, CO_2, N_2 and Ar were chosen as diluents. Their addition has a significant influence. Among the three diluents, CO_2 has the greatest influence on liftoff height, followed by N_2, and then Ar; for example, only 5% of CO_2 can achieve a three times increase of H_L. As shown in Fig.6, the abscissa normalization by $K_{diluent}$ imposes a unique H_L curve for the three diluents under given aerodynamic conditions. This can be still explained through the laminar burning velocity (S_L), a key element in lifted flame stabilization process. According to the work of Qiao et al. (2010), measured and calculated S_L of premixed flames attained an identical value provided that the following relative amount of diluent, equal to 1 : 1.9 : 2.9, was added for CO_2, N_2 and Ar respectively. Their result is consistent with the present values of $K_{diluent}$. Hence identical H_L values were obtained for lifted flames having the same S_L. By using $(Q_{diluent}/Q_{air})/(Q_{diluent}/Q_{air})_{lifting}$ as a reduced abscissa, the superposition of curves obtained with different diluents was already noted in our work (Min et al., 2010) for attached flame concerning their standoff height as well as their OH zone thickness: it was quantified and interpreted as a similarity-law behavior. Moreover, normalizing H_L by its initial value H^o_L eliminates the

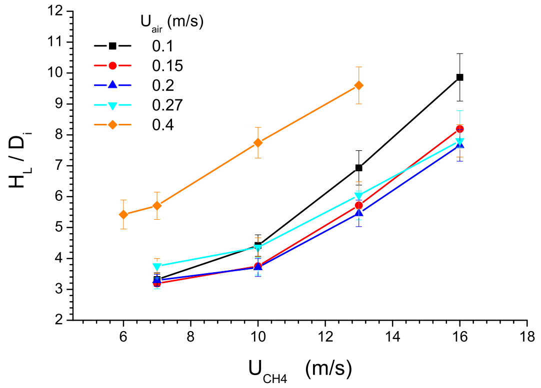

Fig. 5 Evolution of H_L/D_i without dilution

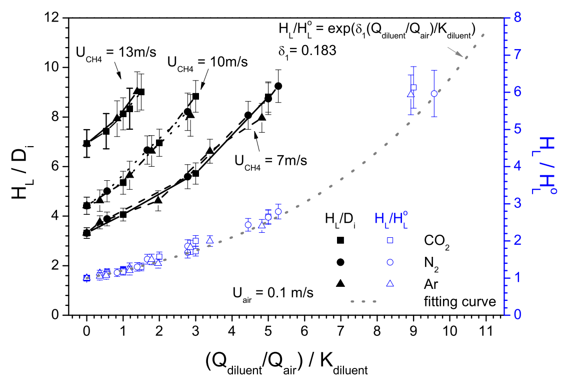

Fig. 6 H_L/D_i vs. $(Q_{diluent}/Q_{air})/K_{diluent}$

shift between curves induced by aerodynamic conditions, and leads to a unique H_L-evolution as a function of the diluent proportion for a given U_{air}. For lifted flames with $H_L < 10D_i$ (1st window) and $21D_i < H_L < 35D_i$ (2nd window), an exponential parametric equation is proposed to describe the global $H_L/H°_L$-evolution: $H_L/H°_L = \exp(\delta_1(Q_{diluent}/Q_{air})/K_{diluent})$, with δ_1 dependent on U_{air}. In this equation, $K_{diluent}$ takes into account the influence of diluent type, while $H°_L$ includes the impact of U_{CH4}.

The apparent flame radius, R_P was extracted from the integrated CH*-chemiluminescence images. Results of R_P, in Fig.7, indicate a systematic radius enlargement when a diluent is added. This expansion can be explained by the following mechanism: as a diluent is added in the air side, lifted flame is pushed backwards as shown by H_L evolution. It ascends by following the stoichiometric line imposed by reactant mixing. First, as the stoichiometric line in a turbulent stream goes outwards along the downstream distance, flame radius is obviously found to be augmented. Second, the position of the stoichiometric line is shifted towards the oxidant side by a diluent addition which diminishes the O_2-concentration. R_P shows a behavior similar to that of H_L: (i) a unique R_P curve for the three diluents as a function of the reduced abscissa, $(Q_{diluent}/Q_{air})/K_{diluent}$; (ii) a global exponential-like R_P-evolution, $R_P/R°_P = \exp(\delta_2 (Q_{dilu\,ent}/Q_{air})/K_{diluent})$, with δ_2 dependent on U_{air} only for lifted flame located inside the first window ($H_L < 10D_i$). Indeed, R_P-data for lifted flames with $H_L > 21D_i$ do not satisfy any more this evolution-law. It shows an over-increase behavior due to a substantial amount of diluent.

Now, results of R_P are plotted vs. the corresponding data of H_L in order to analyse their relative increase. With no-dilution, R_P have been verified to follow a linear evolution as observed by Cessou et al. (2004). With dilution, $R_P/R_P°$-data for lifted flames with $H_L < 10D_i$ evolves against $H_L/H_L°$ as a power-like fitting curve: $R_P/R_P° = (H_L/H_L°)^{0.45}$. This exponential coefficient can be also deduced from the relative ratio between δ_1 and δ_2. Thus, H_L increases more rapidly than R_P, when a diluent is added. Besides, the fact that data collapse on the same curve reveals that one flame radius corresponds to one possible flame stabilisation height, regardless of aerodynamic and dilution conditions. This indicates that lifted flames ascend along the stoichiometric line by following a unique probable path for lifted flames with a $H_L < 10D_i$. On the other hand, for lifted flames with a $H_L > 21D_i$, an apparent shift is observed from the former power-evolution. This implies an overexpansion of flame radius which can be attributed to the methane jet influence: (i) for $H_L < 10D_i$, flame base located in the near field is essentially driven by to the jet mixing layer. Thus, flame base should remain close to the mixing interface of methane and oxidant in order to get a satisfactory mixture and velocity condition; (ii) for lifted flame with a $H_L > 21D_i$, its base stabilizing at the complete mixing region is no longer influenced by the methane jet structure. As a great amount of diluent is demanded to achieve such H_L, the stoichiometric line greatly moves outwards. This explains the over-expansion of flame base.

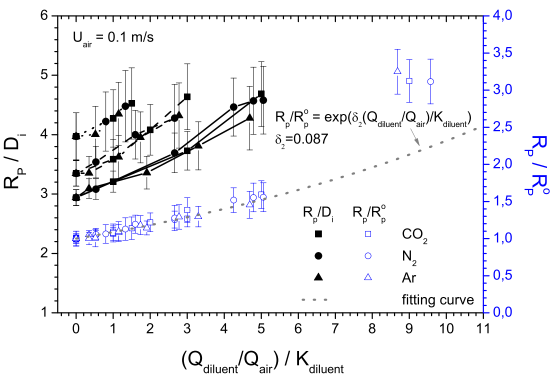

Fig. 7 R_P/D_i vs. $(Q_{diluent}/Q_{air})/K_{diluent}$

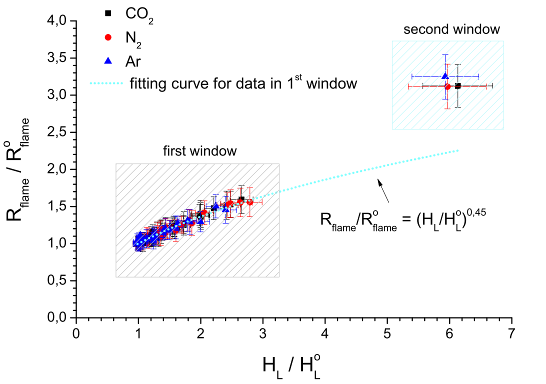

Fig. 8 Correlation between $R_P/R_P°$ and $H_L/H_L°$

5 Conclusion

Flame extinction behavior for air-side diluted non-premixed flames has been extensively investigated within a large range of aerodynamic conditions as well as for four different diluents. In the physical space $(Q_{diluent}/Q_{air}, U_{air}, U_{CH4})$, extinction limits are expressed as a 3D surface $E_{extinction}$. For U_{CH4} >

$U_{CH4,ex}$, extinction limits are described by a characteristic surface which linearly decreases with the increase of U_{air} and is independent of U_{CH4}. It concerns lifted flames for which the burner rim is not involved in stabilization mechanism. For $U_{CH4} \leq U_{CH4,ex,}$ $E_{extinction}$ coincides with the flame lifting surface, $F_{lifting}(Q_{diluent}/Q_{air}, U_{air}, U_{CH4})$. Flames, necessarily attached to the burner can still exist even at a dilution level higher than the former characteristic values due to the wake structure behind the burner rim. As extinction occurs soon after flame lifts off, $E_{extinction}$ partially coincides with $F_{lifting}$. Furthermore, $K_{diluent}$ characterizing the relative order between extinction limits measured with three diluents is the same as that obtained for liftoff limits: $K_{CO2} = 1$, $K_{N2} = 1.9$ and $K_{Ar} = 2.9$, which means CO_2 has the greatest influence, followed by N_2, and then Ar. Unique evolutions obtained with the diluents for H_L and R_P respectively have been found when $(Q_{diluent}/Q_{air})/K_{diluent}$ is used as the normalized abscissa. Indeed, an identical burning velocity (S_L) is obtained provided that the three oxidants are diluted by $(Q_{diluent}/Q_{air})/K_{diluent}$ appearing as a similarity-law quantity. Both H_L and R_P follow an exponential-like evolution. However, an over-increase of flame radius (R_P) is observed on condition that lifted flame stabilized inside the complete mixing region ($H_L > 21D_i$).

Acknowledgement

This work was supported by the French National Research Agency and the Région Haute-Normandie.

References

A. Cessou, C. Maurey, D. Stepowski (2004), 'Parametric and statistical investigation of the behavior of a lifted flame over a turbulent free-jet structure', *Combustion and Flame* **137**, 458-177.

H. Guo, J. Min, C. Galizzi, D. Escudié, F. Baillot (2010), 'A Numerical study on the effects of CO_2/N_2/Ar addition to air on liftoff of a laminar CH4/Air diffusion flame' *Combustion Science and Technology* **182**, 1549 — 1563.

J. Min, F. Baillot A. Wyzgolik, E. Domingues, M. Talbaut, B. Patte-Rouland, C. Galizzi (2010), 'Impact of CO_2/N_2/Ar Addition on the Internal Structure and Stability of Nonpremixed CH4/Air Flames at Lifting', *Combustion Science and Technology* **182**, 1782–1804.

L. Qiao, Y. Gan, T. Nishiie, W.J.A. Dahmb, E.S. Oran. (2010), 'Extinction of premixed methane/air flames in microgravity by diluents: effects of radiation and lewis number', *Combustion and Flame* **157**, 1446-1455.

L. Muniz and M. Mungal (1997), 'Instantaneous flame-stabilization velocities in lifted-jet diffusion flames', *Combustion and Flame* **111**, 16-31.

F. Takahashi and V. Katta (2000), 'A reaction kernel hypothesis for the stability limit of methane jet diffusion flames', *Proceedings of the Combustion Institute* **28**, 2071.

A. Wyzgolik and F. Baillot (2007), 'Response of the non-premixed lifted flame to coaxial jet mixing layers', *Proceedings of the Combustion Institute* **31**, 1583–1590.

A. Wyzgolik and F. Baillot (2009), 'Réponses d'une flamme aux comportements d'un jet coaxial non-prémélangé modulé par acoustique', 'Congrès Français de Mécanique', Marseille.

Y. Otakeyama, T. Tokomori, M. Mizomoto (2009), 'Stability of CH_4-N_2/air jet diffusion flame for various burner rim thicknesses', *Proceedings of the Combustion Institute* **32**, 1091-1097.